Solvation of cyclopentadienyl and substituted cyclopentadienyl radicals in small clusters. I. Nonpolar solvents

J. A. Fernandez, J. Yao, and E. R. Bernstein

Solvation of cyclopentadienyl and substituted cyclopentadienyl radicals in small clusters. I. Nonpolar solvents

J. A. Fernandez, J. Yao, and E. R. Bernstein[a)]
Department of Chemistry, Colorado State University, Fort Collins, Colorado 80523-1872

Cyclopentadienyl (cpd), methylcpd (mcpd), fluorocpd (Fcpd), and cyanocpd (CNcpd) are generated photolytically, cooled in a supersonic expansion, and clustered with nonpolar solvents. The solvents employed are Ar, N_2, CH_4, CF_4, and C_2F_6. These radicals and their clusters are studied by a number of laser spectroscopic techniques: Fluorescence excitation (FE), hole burning (HB), and mass resolved excitation (MRE) spectroscopies, and excited state lifetime studies. The radical $D_1 \leftarrow D_0$ transition is observed for these systems: The radical to cluster spectroscopic shifts for the clusters are quite large, typically 4 to 5 times those found for stable aromatic species and other radicals. Calculations of cluster structure are carried out for these systems using parameterized potential energy functions. Cluster geometries are similar for all clusters with the solvent placed over the cpd ring and the center-of-mass of the solvent displaced toward the substituent. The calculated cluster spectroscopic shifts are in reasonable agreement with the observed ones for N_2 and CF_4 with all radicals, but not for C_2F_6 with the radicals. The Xcpd/Ar data are sacrificed to generate excited state potential parameters for these systems. CH_4 is suggested to react with all but the CNcpd radical and may begin to react even with CNcpd. van der Waals vibrations are calculated for these clusters in the harmonic approximation for both D_1 and D_0 electronic states; calculated van der Waals vibrational energies are employed to assign major cluster vibronic features in the observed spectra. © *1999 American Institute of Physics.* [S0021-9606(99)01210-6]

I. INTRODUCTION

The study of van der Waals (vdW) clusters of stable molecules has enjoyed a good deal of success and has yielded substantial information on the solvation of stable molecules. These results deal with many aspects of cluster properties and behavior: geometry of solvation and solvation sites,[1] solvation or binding energy,[2] rigidity,[1,3] intermolecular vibrations,[4] potential energy surfaces,[5] dynamics[6] (intracluster vibrational energy redistribution—IVR, and cluster vibrational predissociation—VP), and chemistry[7] (e.g., electron transfer, proton transfer, and abstraction and addition reactions). The depth and breadth of these investigations are quite extensive and have often been reviewed.[8]

Comparable results for nonstable, open shell molecules (e.g., radicals, carbenes, nitrenes) would perhaps be even more revealing because one expects the role of solvent to be much more central to the chemical and physical behavior of these systems than for stable closed shell molecules. Nonetheless, relatively few studies involving radicals and clusters can be found in the literature, due in part to the significantly increased difficulties encountered in generating, isolating, cooling, and clustering these short lived, reactive species. Of particular note for cluster studies of radicals are those involving OH–Ne, N_2, H_2,[9] NH, CH–rare gases,[10] CN–Ne,[11] C_2H_3O–Ar,[12] C_5H_5–He, Ne, N_2,[13] $C_5H_4CH_3$–He, Ne,[13] and CH_3O,[14] NCO,[15] and $C_6H_5CH_2$/Ar, N_2, CH_4, C_2H_6, and C_3H_8.[16] Reports involving vdW clusters of aromatic radicals

are limited to the benzyl, cyclopentadienyl, and methylcyclopentadienyl radicals to the best of our knowledge.

In addition to being difficult to access experimentally, radicals and their interactions are also difficult to describe theoretically due to radical reactivity and electronic structure. The cyclopentadienyl (cpd) radical is perhaps the most accessible open shell aromatic radical.[17] The Xcpd (X=H, F, CH_3, CN) radical series is quite rich and a number of interesting observations can be made with these radicals; in particular, the ground state of cpd is degenerate and its Jahn–Teller properties can be explored,[17] and the substituent groups attached to the cpd ring can vary the electronic (electrophilic) nature of the radical with electron withdrawing, electron donating, and resonance stabilization interactions that tune both reactivity toward hydrogen abstraction and solvation interactions.

As part of an ongoing effort to study the reactions and intermolecular interactions of open shell species, we have carried out an extensive investigation of the aromatic family of cyclopentadienyl radicals, XC_5H_4 (with X=H, CH_3 F, CN-cpd, mcpd, Fcpd, CNcpd), clustered with nonpolar solvents. To determine the interactions, binding energies, and ($D_1 \leftarrow D_0$) spectroscopic shifts for these solvated radicals, both experimental and theoretical investigations are performed. Three types of experiments are undertaken for these systems: Fluorescence excitation (FE) spectroscopy, mass resolved excitation (MRE) spectroscopy, and hole burning spectroscopy. The spectroscopic results are analyzed with the aid of *ab initio* quantum chemical and semiempirical atom–atom potential energy calculations. With these approaches

a)Electronic mail: erb@lamar.colostate.edu

we are able to (1) estimate ground-state binding energies, geometries, and van der Waals modes of the clusters; (2) generate potential energy parameters so that geometries, binding energies, van der Waals modes for electronic excited-state (D_1) clusters can be obtained; (3) estimate the validity of this approach to cluster properties; and (4) explore possible explanations for any systematic deviations between theory and experiment that may arise (e.g., reaction or charge transfer). In this present report (the first of a series of three, each dealing with a specific aspect of Xcpd vdW clusters), we analyze the interactions of the four radicals with the non-polar solvents Ar, N_2, CH_4, CF_4, and C_2F_6. The agreement between experimental and theoretical results for all but CH_4 clusters suggests that a good model for these clusters and their spectra can be achieved on both the ground and excited state potential surfaces. CH_4 appears to react with all but CNcpd on the excited state cluster potential surface. The CNcpd(CH_4)$_1$ cluster appears to be commencing a reaction at the D_1 O_0^0 level of excitation.

II. PROCEDURES

A. Experimental

The details of our experimental approach and arrangements have been given in previous publications dealing with radicals and radical clusters.[14–16]

In the fluorescence excitation experiments, a general valve pulsed nozzle is used to generate an adiabatic expansion of the appropriate mixture of molecular precursor for Xcpd (<1% of the total pressure), the solvent gas (0.1%–10% of the total pressure), and 50–400 psi He expansion gas. The stainless steel vacuum chamber into which the mixture is expanded remains at ~10^{-4} Torr during the FE experiment. The precursor molecules for the Xcpd photolytic generation are methylcyclopentadiene dimer for cpd and mcpd, o-fluoroanisole for Fcpd, and phenylazide and phenyl-isocyanate for CNcpd. Phenylazide is synthesized according to Ref. 18. Precursors are placed in a glass boat in the high-pressure gas line just behind the nozzle entrance. Exact concentrations of various precursor species in the expansion mixture depend on the vapor pressure of the sample: Samples are typically kept in the nozzle at <40 °C. Methyl-cyclopentadiene dimer is warmed within this range to generate monomer in the gas phase.

To produce radicals from the precursors, an ArF excimer laser output (193 nm, 80 mJ/pulse, 10 Hz) is aligned col-linearly with the molecular beam axis and focused inside a quartz tube (1 cm×1 mm i.d.) attached to the exit of the nozzle, using a 30 cm focal length lens. A Nd/YAG pumped dye laser system is employed to study the $D_1 \leftarrow D_0$ optical transitions of the radicals and their clusters. The probe laser crosses the molecular beam about 1.5 cm downstream from the exit of the quartz tube. The dyes appropriate for these radicals are DCM (output doubled)-Fcpd, LDS 698+DCM (output doubled)-cpd/mcpd, and R590 (output mixed with 1.064 μm) and F548 (output mixed with 1.064 μm)-CNcpd. Fluorescence is detected in a direction perpendicular to the plane formed by the molecular and laser beams. An RCA C31034A photomultiplier tube is used to detect the emission

from the radicals and their clusters. UV340 (cpd, mcpd, Fcpd) and U360 (CNcpd) glass filters are employed to reduce scattered light from the excimer laser and other species generated in the molecular beam.

Hole burning (HB) experiments are conducted using two separate and identical laser systems with a time delay of 1 μs between them. One laser ($t=1$ μs) remains at a fixed energy to generate a level of fluorescence intensity from a specifically chosen transition of the cluster species. Another laser (four times higher in intensity, $t=0$ μs) is tuned through the other nearby transitions that may or may not belong to the same cluster as the first transition. Transitions arising from the same ground state level as that generated by the fixed frequency laser (cluster of the same mass and structure) will cause the monitored fluorescence intensity to change and thus trace out the same spectrum as a single laser would. Transitions for a different cluster (either structure or mass) and those of the same cluster arising from an excited ground state vibrational mode of the cluster will, of course, not cause a change in the monitored fluorescence generated by the fixed frequency laser and will thus be absent from the HB spectrum.

Mass resolved excitation spectra (MRES) are obtained using an R. M. Jordan pulsed nozzle to expand the above described gas mixtures into a stainless steel vacuum chamber held at 1 to 2×10^{-6} Torr during the experiment. Typical gas expansion pressures for this nozzle and chamber are ~50–150 psi. The $D_1 \leftarrow D_0$ excitation laser for the radical species is the same as described above and a second similar laser is employed for ionization ($l \leftarrow D_1$) of the clusters. The ionization laser uses fluorescein 548, and its output is doubled and then mixed with 1.064 μm radiation to ionize the species studied.

B. Theoretical

A theoretical description of the clusters plays an important role in our understanding of both solvation and chemistry. Four experimental observations can be employed to check the accuracy of the theoretical approach: (1) The cluster spectroscopic shift, the difference between the bare radical transition energy and the cluster transition energy; (2) the cluster binding energies in different electronic states; (3) the cluster equilibrium structure as determined through rotational structure analysis; and (4) the cluster vdW vibrational energies in different electronic states.

A great deal of experience has been accumulated in the last two decades with regard to calculation of these experimental observables based on semiempirical potential energy surfaces for clusters of an aromatic chromophore molecule[1,2,19] solvated by both polar and nonpolar solvent molecules. For example, benzene–rare gas, CH_4, H_2O, NH_3, C_2H_6[2,19] clusters have been studied with regard to structure, binding energy, vdW modes and the calculated results are in good agreement with the experimental data. The cluster structure has, in general, the solvent molecule ring centered. Calculated binding energies are typically sufficient to predict accurate cluster dynamics and spectroscopic shifts. All of these results give great confidence in predictions of cluster

properties based on semiempirical potential energy surface calculations.

Moreover, such calculations have proven their worth for aromatic and nonaromatic radical–solvent molecule clusters. Similar calculations have now been carried out for benzyl radical clusters,[16] and for CH_3O[14] and NCO[15] clusters. Perhaps most impressive is that the calculated structures for CH_3O and NCO clusters agree with those determined from resolved rotational structures for the cluster. These structures were not anticipated from previous experimental results. This important agreement between calculational and experimental results underscores the general predictive nature of the potential energy surface calculations based on semiempirical potentials. Of course, such potentials have a long history of success for the study of crystal structures, vibrational modes, and other intermolecular properties.[20]

A second approach to such calculations should at least be considered and explored. *Ab initio* calculations can be attempted to determine these intermolecular interactions and properties. The difficulty with this algorithm is at least twofold: Very little experience with these closed and open shell system calculations exists so that one cannot have much predictive confidence in the results; and the very high level of calculation that must be employed to determine (relative) energies to ± 0.1 kcal/mol for both open and closed shell structures. Recall also that to fit much of the experimental data, properties for both ground and excited state clusters must be calculated.

Ab initio calculations of cluster structure, binding energy, and intracluster vibrational modes must begin with a large basis set for both heavy and light atoms. We use cc-pVDZ or larger sets for most of our calculations as suggested below for partial atomic charge calculations. This set places *p*-functions on H and *d*-functions on the heavy atoms. Certainly, a post-HF nondensity functional algorithm must be used for the calculation, but a second-order Moller–Plesset (MP2) or MP4 calculation does not account for the static correlation or degeneracy problems that must arise for the cpd cluster systems. Thus, a proper calculation would include a full valence complete active space (CAS) method for the clusters and then MP2 or multireference configuration interaction (MRCI) on that wave function. Even at this level, one has little or no experience with the predicted results and how basis set superposition error will influence them. We are attempting such calculations for small radicals (e.g., NCO, CH_3O, NO_3, CH_3), with small solvents (e.g., CH_4, HCN, CH_3OH, H_2O, etc.), but this work is still in progress. In any event, these calculations will not be of predictive value for experimental results until a number of different systems are studied at a series of basis set and algorithm levels.

Given the above presentation, the results presented in this work will be analyzed and assigned as appropriate through semiempirical potential energy function calculations as described below.

In order to understand and analyze the experimental results, an extensive series of calculations is performed on each solute–solvent system.

Cluster structure is determined by employing a potential

energy calculation, based on atom–atom Lennard-Jones Coulomb potential energy functions,[21]

$$E = \sum_{i=1}^{n} \sum_{j=1}^{m} {}' \left\{ \left(\frac{A_{ij}}{r_{ij}^{12}} - \frac{C_{ij}}{r_{ij}^{6}} \right) (1 - \delta_{ij}^{hb}) + \frac{q_i q_j}{D r_{ij}} \right.$$
$$\left. + \left(\frac{A_{ij}^{hb}}{r_{ij}^{12}} - \frac{C_{ij}^{hb}}{r_{ij}^{10}} \right) \delta_{ij}^{hb} \right\}, \tag{1}$$

in which

$$A_{ij} = C_{ij} r_{\min}^6 / 2 \quad \text{and} \quad C_{ij} = \frac{3/2 e (\hbar/m^{1/2}) \alpha_i \alpha_j}{(\alpha_i N_i)^{1/2} + (\alpha_j / N_j)^{1/2}}. \tag{2}$$

m is the electronic mass, δ_{ij} is 1 when the atoms can form hydrogen bonds and 0 in the rest of the cases, q_i, q_j are the atomic charges for atoms i and j, D is the dielectric constant, $r_{\min}$ is the sum of van der Waals radii r_i, r_j and is different for each pair of atoms, α_i is the atomic polarizability and is evaluated from experimental data, N_i is the effective number of electrons for each atom type, and r_{ij} is the distance between atoms i and j of different molecules. The sums in Eq. (1) are carried out such that interactions are counted only once.

Equation (1) generates a good description of the interactions between the molecules that form a vdW cluster if all the parameters are known; however, values for atomic charges in the Xcpd system are not available in the literature. Moreover, since the experimental information that must be fit to prove the structure and the interactions (cluster spectroscopic shift) involves both ground and excited state cluster binding energies, *ab initio* calculations for atomic charges in both states must be employed to evaluate the appropriate potentials. The ground and excited state Xcpd radical and ground state molecular solvent (N_2, CH_4, CF_4, C_2F_6) atomic charges are calculated using the GAUSSIAN 94 program package.[22] The results are summarized in Table I.

Structures and transition energies (see Table II) are calculated for all radicals as a test of the quality of the calculational level employed. For cpd, mcpd, and Fcpd, the complete active space self-consistent field (CASSCF)(5,5)/cc-pVDZ theory level is found to be quite sufficient. The active space for the CASSCF is formed by all five π-electrons of the ring and the five π-orbitals. For CNcpd, the CN group π electrons are also included in the active space and a CASSCF(9,9)/cc-pVDZ calculation is performed.

Calculation of the atomic charges is a complicated problem that requires careful selection of a basis set and the method employed to isolate charges. In Table III, cpd atomic charges, calculated using different basis sets, are shown. Two different methods are used in the charge determination: Mulliken analysis (columns labeled as ''a'') and a grid method to fit charges to electrostatic potential points[27] (columns labeled as ''b'').

By comparison with other aromatic ring systems, one can expect a charge somewhat larger than -0.1 a. u. for the carbon atoms and approximately $+0.1$ on the hydrogen atoms. These are typical values for molecules such as benzene, benzyl radical, aniline, etc; however, Xcpd radicals have an

TABLE I. Parameters used in the atom–atom potential calculation. Polarizabilities (α_i) in Å^3, charges (q_i) in atomic units, vdW radii in Å. For solvent molecules, see parameters in Refs. 14, 15, and 21.

Radical	Atom	Ground state			Excited state		
		q_i	α_i	r_{ii}	q_i	α_i	r_{ii}
cpd	C1	−0.4446	1.150	3.700	−0.2160	1.341	3.421
	C2=C5	0.1630	1.150	3.700	−0.1003	1.341	3.421
	C3=C4	−0.2257	1.150	3.700	−0.0279	1.341	3.421
	H1	0.1599	0.420	2.930	0.1097	0.420	2.930
	H2=H5	0.0672	0.420	2.930	0.0878	0.420	2.930
	H3=H4	0.1378	0.420	2.930	0.0935	0.420	2.930
mcpd	C$_{Me}$	−0.2303	0.930	4.120	−0.2238	0.930	4.120
	C1	0.3808	1.150	3.700	0.1753	1.370	3.401
	C2	−0.4141	1.150	3.700	−0.1878	1.370	3.401
	C3	0.0112	1.150	3.700	−0.0585	1.370	3.401
	C4	−0.0435	1.150	3.700	−0.1063	1.370	3.401
	C5	−0.3704	1.150	3.700	−0.1536	1.370	3.401
	H2	0.1616	0.420	2.930	0.1051	0.420	2.930
	H3	0.0795	0.420	2.930	0.1002	0.420	2.930
	H4	0.0897	0.420	2.930	0.0898	0.420	2.930
	H5	0.1545	0.420	2.930	0.0675	0.420	2.930
	H6	0.0639	0.420	2.920	0.0793	0.420	2.920
	H8=H9	0.0589	0.420	2.920	0.0565	0.420	2.920
fcpd	F	−0.2456	0.557	3.364	−0.2436	0.557	3.364
	C1	0.5703	1.150	3.700	0.3395	1.341	3.421
	C2=C5	−0.4425	1.150	3.700	−0.2616	1.341	3.421
	C3=C4	−0.0228	1.150	3.700	−0.0227	1.341	3.421
	H2=H5	0.1889	0.420	2.930	0.1376	0.420	2.930
	H3=H4	0.1141	0.420	2.930	0.0987	0.420	2.930
cncpd	N	−0.5178	0.930	3.510	−0.4520	0.960	3.460
	C$_{CN}$	0.4080	1.150	3.700	0.2429	1.220	3.570
	C1	−0.2338	1.150	3.700	0.1182	1.294	3.500
	C2=C5	0.1149	1.150	3.700	−0.2050	1.294	3.500
	C3=C4	−0.1730	1.150	3.700	0.0301	1.294	3.500
	H2=H5	0.1043	0.420	2.930	0.1333	0.420	2.930
	H3=H4	0.1255	0.420	2.930	0.0871	0.420	2.930

TABLE II. Calculated structural parameters for the four radicals. Cpd, mcpd, and fcpd parameters were calculated at CASSCF(5,5)/cc-pVDZ level. CNcpd structure calculated at CASSCF(9,9)/cc-pVDZ level. Distances in Å, energies in cm^{-1}.

Radical	Bond	Ground state		Excited state		Transition energy	
		This work	Other work	This work	Other work	Exp.	Calc.
cpd	R_{CC}	1.420	1.421[a]	1.457	1.447[f]	29 573.3	28 617
	R_{CH}	1.079	1.077[b]	1.077	1.080[f]		
mcpd	R_{12}	1.445	1.437[b]	1.457	1.445[c]	29 765.3	30 590
	R_{23}	1.370	1.378[b]	1.370	1.445[c]		
	R_{34}	1.482		1.458			
	$R_{C–Me}$	1.497	1.501[b]	1.496	1.504[b]		
	$R_{H2C–H}$	1.092	1.093[c]	1.093	1.093[c]		
	R_{CH}	1.080	1.083[c]	1.078	1.069[c]		
Fcpd	R_{12}	1.428	1.503[b]	1.443	1.440[b]	30 758.2	31 589
	R_{23}	1.373		1.461			
	R_{34}	1.483		1.456			
	$R_{C–F}$	1.316	1.283[b]	1.320	1.298[b]		
	R_{CH}	1.078		1.076			
CNcpd	R_{12}	1.448	1.442[b]	1.457		27 144.6	29 057
	R_{23}	1.366	1.365[b]	1.444			
	R_{34}	1.487		1.466			
	$R_{C–CN}$	1.425	1.411[b] 1.451[d]	1.405	1.377[b]		
	R_{CN}	1.164	1.158[b]	1.173			
	R_{CH}	1.078	1.094[e]	1.076			

[a] Reference 23.
[b] Reference 17.
[c] Reference 17.
[d] Reference 24
[e] Reference 25.
[f] Reference 26.

unpaired electron on the ring so the charges on each carbon atom can be larger than for stable molecules.

The cpd ground state charge distribution given in Table III generates C_{2v} symmetry, even though the molecular geometry is forced to be D_{5h}. This is due to the electronic configuration. The half-filled orbital has a C_{2v} symmetry, and this probably determines the charge distribution for the carbons. The barrier for the rotation of the C_{2v} geometry around the ring is very small,[17] and the result is an ''effective'' D_{5h} geometry. The mean of charges for all the carbons of the ring is employed instead of the particular values; of course, the same is true for the hydrogens, $q_C = -q_H$. For the rest of the radicals, the substitution fixes the radical electron at the substituted carbon (C_1), leading to a C_{2v} symmetry for the ring charge distribution.

Table III also demonstrates that increasing the basis set complexity does not lead to a converged value for the charges if the Mulliken population analysis procedure is employed to generate them. Also the jump from a 6-31++G** to a cc-pVDZ leads to a completely different charge distribution within this approach. If a grid/potential procedure is used (columns labeled ''b''), the results from the calculations with the three smaller basis sets are not consistent with the shape of the half-filled orbital (with a large electron density in the carbons 1, 4, and 5), but if polarized

functions are taken into account on the Hs (indicated by a second star), the charge distribution adopts a shape closer to that expected. Moreover, as the basis set size is increased, the charge distribution tends to a limiting value, independent of the basis set employed. As no difference is evident between the charge distributions obtained with 6-31G**, 6-31++G** and cc-pVDZ for cpd, we employ the 6-31G** basis set in the calculation of the rest of the radical atomic charges. The charges employed, together with the rest of the parameters, are shown in Table I. We estimate that parameter errors could be as large as ~±10%.

To reproduce the experimental cluster spectroscopic shifts, excited state binding energies must also be calculated, but excited state values for q_i, α_i, and r_i are not found in the literature. To solve this problem and obtain excited state cluster binding energies we estimate the atomic polarizabilities and vdW radii for each excited state radical, using the Xcpd(Ar)$_1$ cluster shift data (see Ref. 16 for a detailed description of the process). As a guide for this procedure, we consider that the atoms whose charges change more upon electronic excitation will also experience the largest change in their other parameters, due to the relationship between atomic charges, polarizabilities, and vdW radii. Additionally, we assume that the H atoms are not much affected by the electronic excitation. Thus, we assume that upon electronic excitation, only the radical carbon parameters change. For mcpd, the CH$_3$ group will not be affected by the excitation of

TABLE III. Calculated charges (in atomic units) for cpd radical, using a) Mulliken population analysis and b) potential grid. The charge calculation is carried out at CASSCF/6-31G** level using the structure found at CASSCF/cc-pVDZ level. The active space is formed by the 5· electrons of the ring and the five π and π^* orbitals.

Ground state	6-31G		6-31G*		6-31+G*		6-31G**		6-31++G**		cc-pVDZ	
	a	b	a	b	a	b	a	b	a	b	a	b
C1	−0.1624	0.1645	−0.1623	0.1534	−0.1286	0.1772	−0.2071	−0.4446	−0.3412	−0.4667	−0.0899	−0.4585
C2	−0.2361	−0.3255	−0.2346	−0.3258	−0.3183	−0.3370	−0.1037	0.1630	0.0278	0.1920	0.0230	0.1813
C3	−0.1893	−0.0020	−0.1884	−0.0178	−0.1992	−0.0057	−0.1730	−0.2257	−0.2102	−0.2267	−0.0531	−0.2295
H1	0.2106	0.0616	0.2029	0.0661	0.2377	0.0594	0.1379	0.1599	0.1295	0.1570	0.0174	0.1592
H2	0.1956	0.1343	0.1950	0.1428	0.2282	0.1398	0.1592	0.0672	0.1476	0.0587	0.0382	0.0616
H3	0.2057	0.0803	0.2046	0.090	0.2347	0.0847	0.1522	0.1378	0.1404	0.1309	0.0308	0.1362
Average C charge		−0.0981		−0.1068		−0.1016		−0.1140		−0.1072		−0.1110
Excited state												
C1	−0.2009	−0.0939	−0.2035	−0.0923	−0.2364	−0.0868	−0.1850	−0.2160	−0.2271	−0.2252	−0.0700	−0.2096
C2	−0.2005	−0.0782	−0.2028	−0.0778	−0.2354	−0.0719	−0.1767	−0.1003	−0.1653	−0.0767	−0.0563	−0.0880
C3	−0.2007	−0.081	−0.2033	−0.0802	−0.2359	−0.0732	−0.1190	−0.0279	−0.0930	−0.0215	0.0063	−0.0295
H1	0.2007	0.0871	0.2032	0.0860	0.2359	−0.0802	0.1378	0.1097	0.1378	0.1023	0.0187	0.1030
H2	0.2007	0.0815	0.2031	0.0809	0.2358	0.0747	0.1494	0.0878	0.1466	0.0759	0.0293	0.0808
H3	0.2007	0.0810	0.2031	0.0803	0.2359	0.0737	0.1698	0.0935	0.1564	0.0838	0.0463	0.0900
Average C charge		−0.0824		−0.0817		−0.0754		−0.0945		−0.0843		−0.0963

the ring, and the same atomic parameters for the CH_3 group atoms are used in both electronic states. The same consideration can be made for Fcpd and the fluorine atom. The effect of both groups will be to add or withdraw electron density from the ring, and to a good approximation, they will affect both states in the same way. [Note that the transition 0_0^0 energies for the three radicals (cpd, Fcpd, and mcpd) are at $\sim 30\,000 \pm 600$ cm^{-1} (see Fig. 1)]. On the other hand, the CN group will be significantly affected by electronic excitation, due to the resonance between the CN triple bond and the ring. To estimate the excited state parameters for this case,

we take into account which atomic charges change more upon excitation and assume that the other atomic parameters for these atoms are also more affected. The resulting parameters are shown in Table I.

Finally, the vdW modes of the cluster are determined by a normal coordinate analysis of the cluster employing the FG matrix method of Wilson et al.[28] Assuming that intramolecular vibrations are not coupled to the low-frequency intermolecular modes, this calculation will generate all the intermolecular vibrations and their eigenvectors in the harmonic approximation for both electronic states of the radicals. We have published[4] the two algorithms we employ to calculate van der Waals modes of clusters and demonstrated the effectiveness of this approach. Both methods generate the same eigenvectors and eigenvalues. These methods ensure that the van der Waals modes are calculated at the proper cluster equilibrium conformation for which all torques and forces on the molecules and atoms are zero. A number of examples are given in Refs. 4, 19, 28, for closed shell systems and in Refs. 14–16 for open shell systems. One of the methods calculates van der Waals modes for fixed molecular geometries and the other calculates van der Waals modes following relaxation of the molecular geometry caused by the intermolecular potentials or forces. The results will be influenced by the accuracy of the geometry calculation, but this calculation is a reasonable starting point from which to assign cluster spectra.

III. RESULTS

A. Bare radicals

Figure 1 shows the spectra of the four Xcpd radicals under consideration. cpd and mcpd have $D_1 \leftarrow D_0$ transitions ($^2A_2'' \leftarrow {}^2E_1''$ for cpd and $^2B_1 \leftarrow {}^2B_1$ for mcpd)[29] within ~ 200 cm^{-1} of one another, while the Fcpd transition is +1200 cm^{-1} higher in energy than that for cpd and the CNcpd tran-
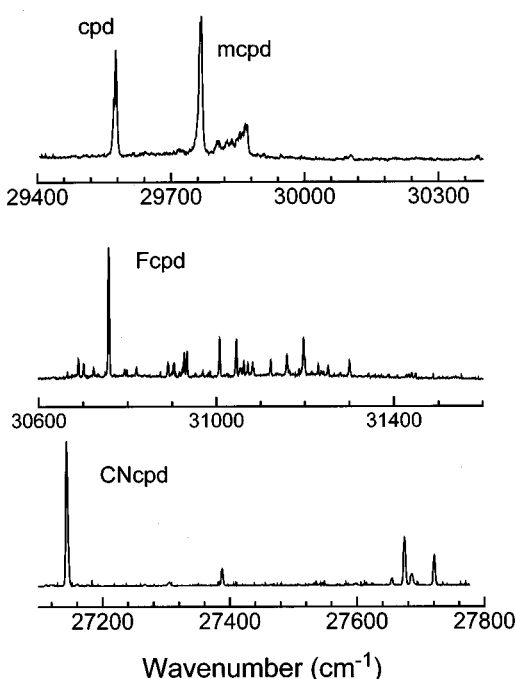

FIG. 1. Fluorescence excitation spectra of cpd, mcpd, Fcpd, and CNcpd.

sition is -2400 cm^{-1} below that for cpd. Almost all the intensity in these transitions is found in the 0_0^0 feature. This absence of vibronic intensity away from the origin can be associated with two phenomena. First, the Franck–Condon factors for this transition clearly favor the origin intensity as can be readily seen in Table II. The ground and excited state geometries are quite similar. Second, as noted by Di Mauro *et al.*[30] previously, the lifetimes of the excited vibronic states that are observed are much shorter than the origin lifetime. For example, for Fcpd the 0^0 state has a lifetime (measured in fluorescence) of 150 ns, while the state at (0_0^0 $+335$ cm^{-1}) has a lifetime of 36 ns. Presumably higher states have much shorter lifetimes. The spectra displayed in Fig. 1 are taken with a narrow time window, which tends to reduce the relative intensity of the origin with respect to the higher vibronic features. If a 150 ns window is used to collect these spectra, the ratio $l(0_0^0)/l(\text{vibronic})$ is even much larger than shown in Fig. 1.

Exactly why this lifetime shortening is observed is not clear. For most aromatic radicals (e.g., Xcpd, benzyl, xylyls) the observed D_1 state is the first excited state, and at 20 000–30 000 cm^{-1} above the ground state the density of coupled D_0 states should be large and fairly constant. Calculations suggest that the next doublet state is more than 5000 cm^{-1} to higher energy and that the lowest quartet state is even higher in energy.

Detection of these radicals through mass resolved excitation spectroscopy has proven difficult, probably due to a small ionization cross section; nonetheless, the mass detected spectrum for CNcpd (ionization energy 72 993 cm^{-1}) is obtained along with that for CNcpd(Ar)$_1$. At least part of the difficulty with this latter detection scheme is that the photolysis process (193 nm light) used to generate these radicals causes a great deal of precursor fragmentation, and the Xcpd signal-to-background ratio approaches 1:1 for high excimer laser power. Additionally, the ionization laser must be focused to create sufficient ion signal and it too can generate ion fragmentation. The concomitant loss of information on these radicals and clusters is partially addressed through hole burning (HB) experiments.

B. CNcpd/Ar, N$_2$, CH$_4$, and C$_2$F$_6$ clusters

CNcpd clusters present rich, intense spectra as can be seen in Figs. 2–5. To distinguish between cluster and bare radical peaks, to test for the existence of more than one cluster configuration, and to identify hot band features, HB spectra are also obtained.

1. CNcpd(Ar)$_1$

The spectrum of the CNcpd(Ar)$_1$ cluster is given in Fig. 2. The origin of the $D_1 \leftarrow D_0$ transition for CNcpd(Ar)$_1$ is at 27 052.6 cm^{-1}. The two most evident features of this spectrum are the large cluster spectroscopic shift [$E(\text{cluster} 0_0^0)$ $-E(\text{radical} 0_0^0)$—see Table IV] and the large number of apparent cluster vibronic features. This is common for nearly all of the cluster spectra reported in this study. Figure 6 gives the calculated ground state structure for the CNcpd(Ar)$_1$ cluster. The argon atom coordinates to the ring π-system at a distance of ~ 3.46 Å, and is displaced from the ring center
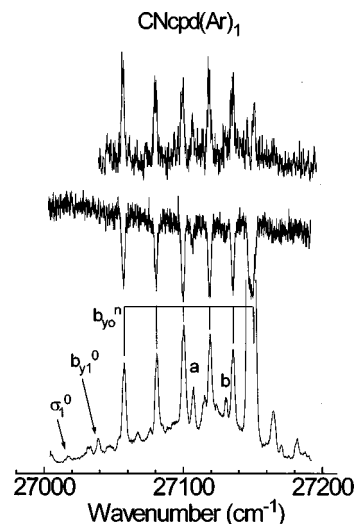

FIG. 2. Fluorescence excitation (lower trace), hole burning (middle trace), and mass (upper trace) spectra of CNcpd(Ar)$_1$. A tentative vdW mode assignment is presented. The features labeled as *a* and *b* are assigned as the cluster σ_0^1 and $b_{y_0}^1 \sigma_0^1$ vibronic transitions, respectively.

toward the CN group. Only one minimum energy structure is found for this cluster; the Ar atom can move above the ring with little change in energy for roughly ± 0.25 Å. These calculations are in agreement with the HB spectra also presented in Fig. 2. These structures is quite similar to those found for both open and closed shell aromatic systems clustered with Ar.[16]

This cluster is employed, as explained in Sec. II B, to determine the CNcpd excited state potential energy function parameters given in Eq. (1). The large red shift observed suggests that dispersion forces (here in the Lennard-Jones form) play a significant role in the cluster binding energy as the Coulomb term is zero for this cluster.

As can be seen in Table V, the assignment of the vdW vibrational modes of the clusters cannot be based solely on
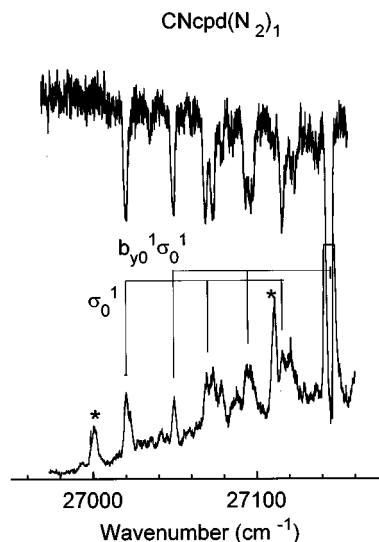

FIG. 3. Fluorescence excitation (lower trace) and hole burning (upper trace) spectra of CNcpd(N$_2$)$_1$. A tentative vdW mode assignment is presented. The features labeled with asterisks correspond to the bare radical peaks.
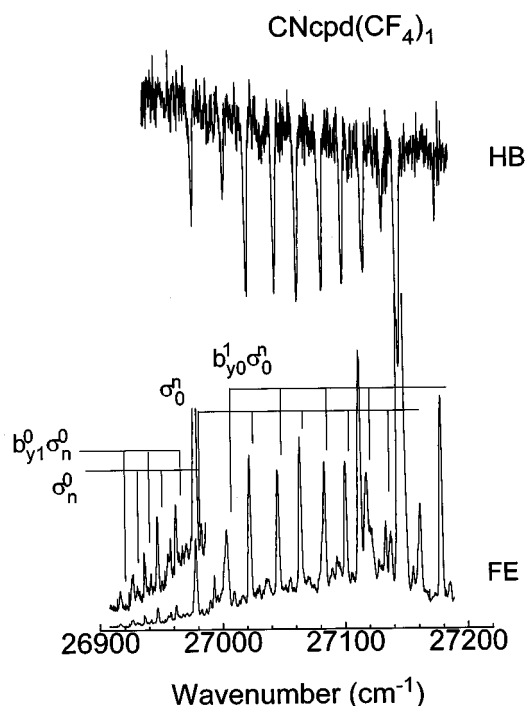
FIG. 4. Fluorescence excitation (lower trace) and hole burning spectra of the $CNcpd(CF_4)_1$ cluster. A tentative cluster vibronic assignment is presented.

TABLE IV. Comparison between calculated and experimental shifts, together with binding energies (in cm^{-1}) for all the clusters studied.

Radical	Solvent		Ground state	Excited state[a]		Shift[b]	
				$p1$	$p2$	Cal.	Exp.
cpd	Ar		358	357	483		−122.1
	N_2		485	466	662	−177	−166.8
	CH_4		460	458	624	−164	
	CF_4		811	790	1035	−224	−179.5
	C_2F_6	1	791	783	1015	−224	−61.0
		2	705	691	907	−202	
mcpd	Ar		402	400	541		−135.1
	N_2		526	506	681	−155	−156.3
	CH_4		527	523	708	−181	
	CF_4		889	866	1036	−147	−143.4
	C_2F_6	1	891	866	1123	−232	−60.2
		2	790	777	1014	−224	
Fcpd	Ar		371	370	497		−126.1
	N_2		469	455	610	−141	−164.5
	CH_4		476	474	641	−165	
	CF_4		793	776	1018	−225	−238.1
	C_2F_6	1	793	786	1012	−219	−52.3
		2	715	702	916	−201	
CNcpd	Ar		398	397	490		−92.0
	N_2		502	477	589	−87	−123.6
	CH_4		518	516	640	−122	−184.3
	CD_4						−150.0
	CF_4		858	839	1025	−173	−167.3
	C_2F_6	1	900	887	1068	−168	−65.3
		2	789	784	950	−161	

[a]$p1$: Calculated using ground state α_i and r_i, but excited state charges and structures; $p2$: Calculated using excited state α_i and r_i, together with excited state charges and structures.
[b]Cal.=calculated shift=(ground state calculated binding energies)$-p2$.

the agreement between theory and experiment, as the calculated values do not always match those observed as well as might be hoped. The problem here is probably twofold: (1) The actual potential is quite flat near the bottom of the well and not very harmonic; and (2) the excited state surface, which is generated to fit the $Xcpd(Ar)_1$ cluster shift in the form of Eq. (1), contains errors from both electronic state
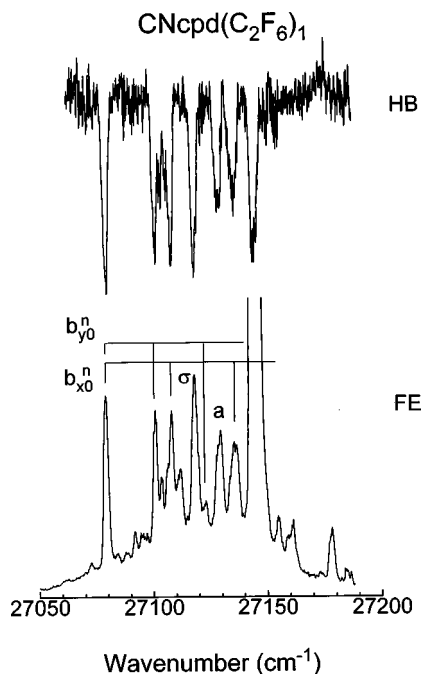

FIG. 5. Fluorescence excitation (lower trace) and hole burning spectra of the $CNcpd(C_2F_6)_1$ cluster. A tentative cluster vibronic assignment is presented. The feature labeled as a is assigned as $b^1_{x_0} b^1_{y_0}$.

potential energy surfaces. We thus base the vdW mode assignment on four principles: (1) C_s totally symmetric modes (σ, the z-stretch, and b_y, the y axis translation, in practice) will form the more intense vibronic progressions for a given spectrum; (2) the calculation does get the proper order for the vibrational energies as $E(b_y) < E(b_x) < E(\sigma)$; (3) displacement of the solvent species over the ring should be in the $+y$ ($X - C_1$) and z directions upon electronic excitation; and (4) in general, the calculation of the σ mode energy in the cluster excited state is typically high by roughly 30%.

Keeping the above in mind, we assign the progressions of peaks with spacing 23.5, 19.5, 18.7, and 16.9 cm^{-1} in Fig. 2 as b^n_{y0} ($n=1-4$). The feature at 49.9 cm^{-1} (labeled in Fig. 2 as "a") can be assigned as due to σ, and the peak at 72.3 cm^{-1} from the cluster origin as $b^1_{y0}\sigma^1_0$. This assignment is also consistent with the expected Franck–Condon factors. The solvent molecule is expected to have a shift in the y and z axes from ground to excited states, due to the differences in the Ar–CN interaction. The x axis position of the solvent molecule should change little in the excitation. This is exactly the case for the calculated excited state cluster structure of $CNcpd(Ar)_1$; moreover, all the other $Xcpd(Ar)_1$ behave in a nearly identical manner upon electronic excitation.

The two peaks to the red of the origin, at 19.0 and 39.6 cm^{-1} can be assigned as b^0_{y1} and σ^0_1, respectively.
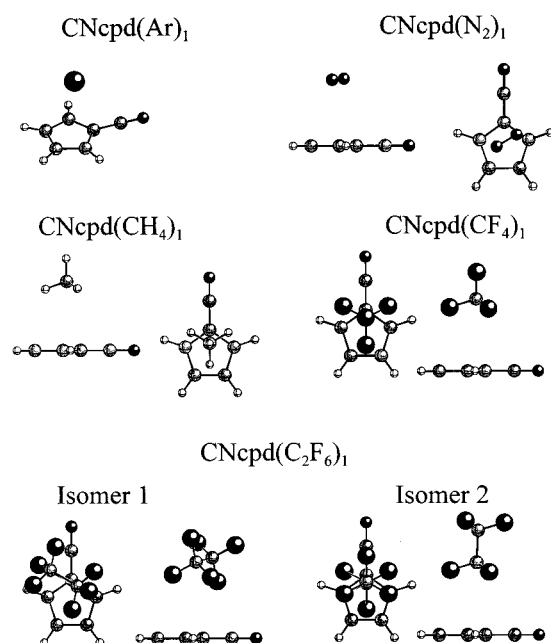
CNcpd(Ar)$_1$ CNcpd(N$_2$)$_1$

CNcpd(CH$_4$)$_1$ CNcpd(CF$_4$)$_1$

CNcpd(C$_2$F$_6$)$_1$

Isomer 1   Isomer 2

FIG. 6. Calculated structures for CNcpd clustered with Ar, N$_2$, CH$_4$, CF$_4$, and C$_2$F$_6$. CNcpd(C$_2$F$_6$)$_1$ is the only system that presents two possible isomers.

2. CNcpd(N$_2$)$_1$

One of the weakest cluster spectra for this system is that belonging to CNcpd(N$_2$)$_1$, as shown in Fig. 3. Because these features are so weak, two CNcpd hot bands also appear in the cluster spectra; they are identified through hole burning studies, as can be seen in Fig. 3. Again the cluster spectrum is quite rich; most main features are composed of doublets or triplets, due to the rotational levels associated with N$_2$ rota-

TABLE V. Comparison between calculated and experimental vdW vibrational energies (in cm^{-1}) for the excited electronic state of the cluster. Ground state modes are indicated by X.

Radical	Solvent		σ Calc.	σ Exp.	b_x Calc.	b_x Exp.[a]	b_y Calc.	b_y Exp.[a]
cpd	Ar		56	46.8	34		34	
	N$_2$		71	55	37		32	
	CF$_4$		71	44.4	15		29	
	C$_2$F$_6$		66		30		23	
mcpd	Ar		57	51	34	(31.6)[b]	23	(31.6)[b]
	N$_2$		76	56	36		24	
	CF$_4$		69	46	28		23	
	C$_2$F$_6$		61		28		26	
fcpd	Ar		56	47.7	33		23	
	N$_2$		74	56	30		22	
	CF$_4$		68	48.2	24		15	
	C$_2$F$_6$		59	41.7	26	(25)[b]	19	(25)[b]
cncpd	Ar	A	54	49.9	32		17	23.5
		X	47	39.6	27		13	19
	N$_2$		70	49	29		17	29
	CH$_4$		90		36	52	17	28
	CF$_4$	A	64	44	31		20	25
		X	57	31	30		14	16
	C$_2$F$_6$		56	39.2	32	28.8	24	21.7

[a]Numbers in parentheses are tentative assignments.
[b]Assignment to bending is clear, but b_x or b_y is not.

tion above the ring about the cluster z (out of the molecular plane) axis.[13(b)] The HB spectrum demonstrates that this additional structure is real and that only one cluster conformer exists. The cluster origin lies at 27 021 cm^{-1}.

The spectroscopic shift for CNcpd(N$_2$)$_1$ is -123.6 cm^{-1}. The calculated shift is large (-87 cm^{-1}) but is still considerably smaller than the observed one (see Table IV). Since the other calculated shifts for N$_2$ solvated Xcpd radicals are in much better agreement with experimental ones than that for CNcpd, we have no explanation for this lack of agreement.

The calculated structure for CNcpd(N$_2$)$_1$ is shown in Fig. 6. The N$_2$ molecule is above the ring with its bond axis parallel to it at ~ 3.33 Å. The N$_2$ molecule is displaced toward the CN group as is the Ar atom for the CNcpd(Ar)$_1$ cluster. The vdW vibrations for the CNcpd(N$_2$)$_1$ clusters can be assigned as a progression in σ built on both the origin and b_y at $0_0^0 + 25$ cm^{-1} and rotational levels of N$_2$ associated with these transitions. The calculated value of b_y is 17 cm^{-1}. The calculation overestimates the energy of the stretching mode by roughly 30%.

3. CNcpd(CF$_4$)$_1$

Figure 4 presents the spectrum of CNcpd(CF$_4$)$_1$. The origin of this spectrum lies at 26 977.4 cm^{-1}. The cluster vibronic spectrum consists of two progressions in a mode at ~ 45 cm^{-1}, one built on the 0_0^0 and the other built on the $0_0^0 + 25$ cm^{-1} feature. The HB spectrum shows that both progressions arise from the 0_0 level and can be associated with a single isomer. Hot band features allow ground state vibrational modes to be identified and assigned as well. The cluster shift in this instance is quite large and negative, -167.3 cm^{-1}. The observed vdW modes are assigned to σ ~ 45 cm^{-1} and $b_y \sim 25$ cm^{-1} and are summarized in Table V.

The cluster calculated structure is depicted in Fig. 6. The CF$_4$ molecule is coordinated to the aromatic CNcpd ring nearly directly over C$_1$, the carbon to which the CN group is attached. Three F atoms coordinate to the ring π-system and one points away from it. The latter C–F bond is parallel to the cluster z axis. One of the fluorine atoms close to the ring is away from the CN–C$_1$ direction ($+y$), and the two other fluorine atoms close to the ring lie on either side of the CN–C$_1$ bond. These two fluorine atoms extend beyond the cpd ring system and appear to be coordinating to the C≡N portion of the π-system of CNcpd. The binding energy for CNcpd(CF$_4$)$_1$ is more than a factor of 2 larger than that for CNcpd(Ar)$_1$. Both the large electron density on the fluorines and their charge contribute to the substantial binding energy. The calculated cluster shift for CNcpd(CF$_4$)$_1$ is -173 cm^{-1} and is in excellent agreement with the observed shift of -167.3 cm^{-1}. The vibrational assignments given in Fig. 4 and Table V ($b_y \sim 25$ cm^{-1} and $\sigma \sim 45$ cm^{-1}) are consistent with guidelines stated for vibrational assignments above.

4. CNcpd(C$_2$F$_6$)$_1$

The spectrum of the CNcpd(C$_2$F$_6$)$_1$ cluster is presented in Fig. 5. The spectroscopic shift for this cluster is the smallest of those reported in this study: The cluster 0_0^0 lies at
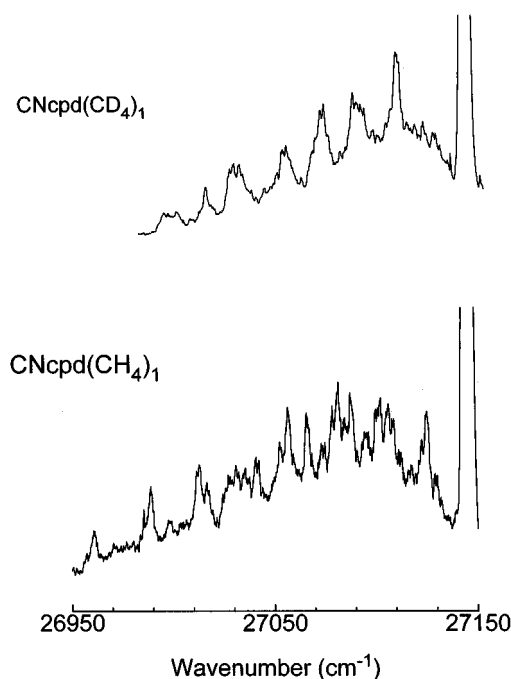
FIG. 7. Fluorescence excitation spectra of CNcpd(CH$_4$)$_1$ and CNcpd(CH$_4$)$_1$.
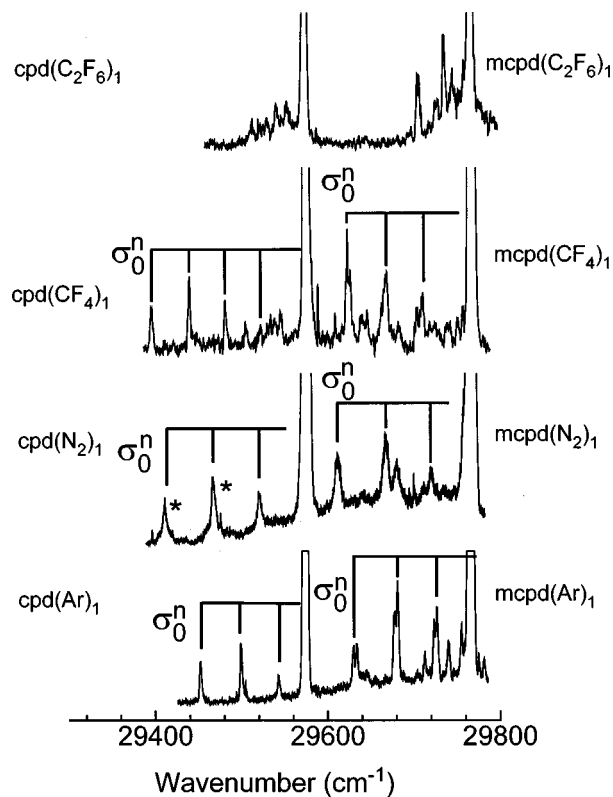

FIG. 8. Fluorescence excitation spectra of cpd and mcpd clusters with Ar, N$_2$, CH$_4$, CF$_4$, and C$_2$F$_6$. A tentative cluster vibronic assignment is presented. Asterisks indicate features arising from contortional motion of N$_2$ over the cpd ring.

27 079.3 cm^{-1} and thus the spectroscopic shift is -65.3 cm^{-1}. All features in the cluster spectrum arise from the same ground state level and thus, from a single isomer.

Structure calculations give two isomers for this cluster: One with C$_2$F$_6$ lying with its C–C axis parallel to the CNcpd ring plane, and the other with one CF$_3$ group coordinated to the ring π-system and the other one away from ring π-system, with the C–C axis perpendicular to the ring. These structures are depicted in Fig. 6. The more stable structure is the former by roughly 100 cm^{-1} (900 vs 789 cm^{-1}). Apparently only the more stable one is found in the supersonic expansion. These structures are reminiscent of those found for benzene and toluene solvated by ethane.[1,31]

The calculated shift for this cluster is roughly structure independent and is about three times larger than that observed. One possible reason for this lack of agreement for the calculated and experimental shifts is that, for this large solvent molecule, the hydrogen atoms of cpd can no longer be considered unaffected by the electronic excitation (see Fig. 6), as they are reasonably close to the fluorine atoms of the solvent ($\sim$3.1 Å.)

Based on the discussion for the vdW mode vibrational assignment presented above, Table V and Fig. 5 present the best estimates of possible observed modes. The assigned modes are b_y (at 22 cm^{-1}), b_x (at 29 cm^{-1}), σ (at 39 cm^{-1}), $[b_x+b_y]$ (at 50 cm^{-1}) and b_x^2 (at 58 cm^{-1}).

5. CNcpd(CH$_4$)$_1$

CNcpd(CH$_4$)$_1$ is the only Xcpd–methane cluster identified in this study: For reasons to be discussed in the next section, other Xcpd(CH$_4$)$_1$ or Xcpd(CD$_4$)$_1$ could not be detected by excitation or pump–probe techniques on the ns time scale. Figure 7 shows the spectra of CNcpd(CH$_4$)$_1$ and (CD$_4$)$_1$. The spectroscopic shift for the CH$_4$ cluster is quite

large, -184.3 cm^{-1}, and for the CD$_4$ cluster the apparent shift is approximately -150 cm^{-1}. This apparent isotopic effect on the shift of $\sim$35 cm^{-1} must surely be due to missing features in the CD$_4$ cluster's spectrum that are lost in the broad underlying background both cluster spectra display. The spectra are quite crowded for this system, due partly to internal rotation of CH$_4$ or CD$_4$ and combinations and overtones. As expected, the internal rotor features are far better resolved for CH$_4$ than for CD$_4$ cluster spectra.

The calculated structure for the CNcpd(CH$_4$)$_1$ cluster is quite similar to that described for CNcpd(CF$_4$)$_1$ as shown in Fig. 6. The solvent is coordinated to the ring π-system but displaced toward the CN substituent and nearly over C$_1$ with a binding energy of 518 cm^{-1} in the radical ground state. Three of the four hydrogens of CH$_4$ are close to the ring and the barrier to internal rotation of the methane about the CH bond parallel to the cluster z axis is small. The calculated cluster shift is -122 cm^{-1}, which is about 50% too small.

C. cpd/Ar, N$_2$, CF$_4$, and C$_2$F$_6$ clusters

cpd clustered with Ar, N$_2$ CF$_4$, and C$_2$F$_6$ displays much sparser and weaker cluster spectra than those for the comparable CNcpd species. HB spectra are too weak for these clusters to be definitively useful. As shown in Fig. 8, cluster spectra for both mcpd and cpd are obtained together due to the proximity of the two radical 0$_0^0$ transitions. In this section we discuss cpd cluster spectra and in the following one we discuss mcpd cluster spectra.
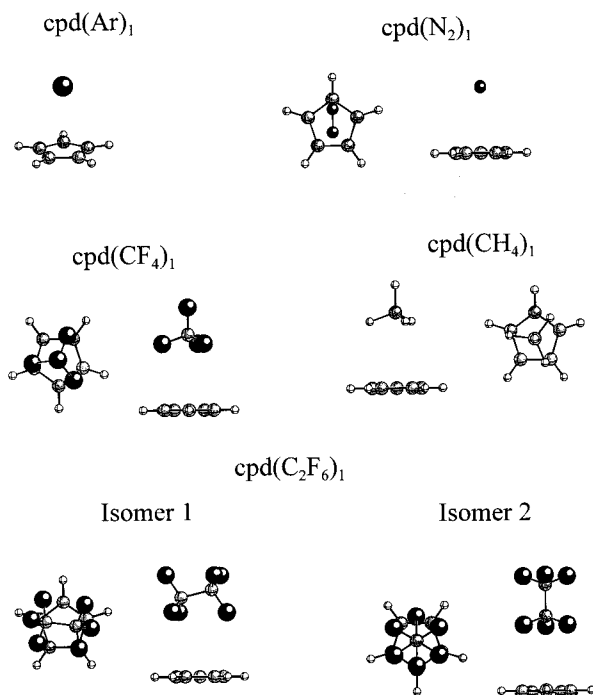
FIG. 9. Calculated structures for cpd clusters with Ar, N_2, CH_4, CF_4, and C_2F_6. cpd(C_2F_6)$_1$ is the only system that presents two possible isomers.

FIG. 10. Calculated structures for mcpd clusters with Ar, N_2, CH_4, CF_4, and C_2F_6. mcpd(C_2F_6)$_1$ is the only system that presents two possible isomers.

Figure 8 depicts spectra of cpd(Ar)$_1$, $(N_2)_1$, $(CF_4)_1$, and $(C_2F_6)_1$ clusters: The origins for the $D_1 \leftarrow D_0$ transitions of these clusters lie at 29 451.2, 29 406.5, 29 393.8, and 29 512.3 cm^{-1}, respectively. The cluster shifts for these species are given in Table IV. The shifts for cpd(Ar)$_1$ and cpd(N_2)$_1$ are quite large (-123.1 and -166.8, respectively) compared to those for the comparable CNcpd clusters. The shifts for the CF_4 and C_2F_6 clusters are similar to those for the comparable CNcpd clusters.

The calculated ground state structures for these clusters are presented in Fig. 9. The basic structure here is as expected: The solvent species lie over the ring center, placed symmetrically, and coordinated to the π-system of the radical. The barriers for rotation of the solvent molecule about the cluster z axis are low for N_2, CH_4, and CF_4.

The cpd(C_2F_6)$_1$ cluster has two possible calculated conformers with binding energies that are quite similar (791 and 705 cm^{-1}). By comparison with other clusters, we suggest that only one isomer is present in the expansion and that this isomer is probably the one with the larger calculated binding energy (isomer 1, with the C_2F_6 C–C bond axis parallel to the cpd ring plane).

The calculated cluster shifts for cpd(N_2)$_1$ and cpd(CF_4)$_1$ are in reasonable agreement with those observed as given in Table IV. The calculated shift for cpd(C_2F_6)$_1$ is nearly a factor of 4 too large. Apparently some interaction term or potential component that reduces the red shift expected from our shift analysis procedure (as discussed above) has been omitted from consideration for the C_2F_6 solvent, as all Xcpd(C_2F_6)$_1$ clusters have roughly the same calculated shift errors as found for CNcpd and cpd clusters. This consistent difference between the calculated and experimental values
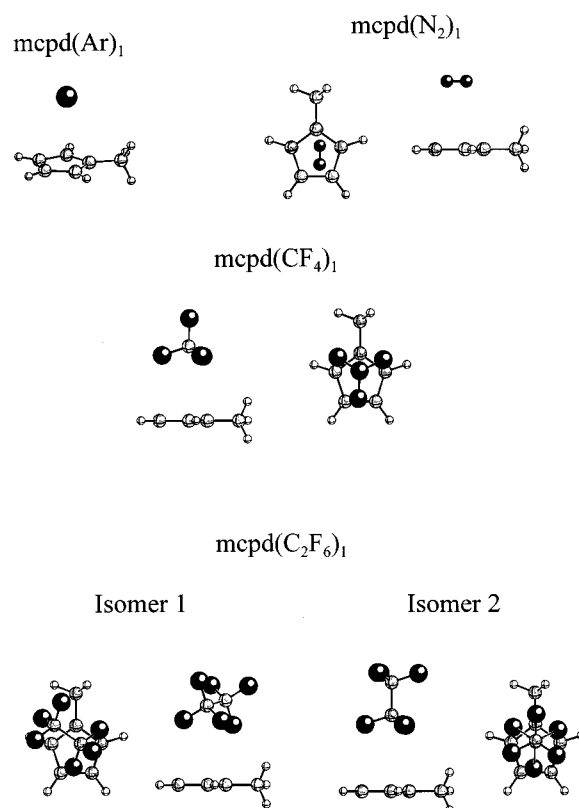
for the Xcpd(C_2F_6)$_1$ cluster shifts, in general, is both remarkable and surprising.

vdW mode progressions that are quite harmonic can be identified for nearly all of the clusters and correspond to the totally symmetric z axis stretch mode σ. These are indicated in Fig. 8 and Table V.

D. mcpd/Ar, N_2, CF_4, and C_2F_6 clusters

Figure 8 shows that the mcpd clusters have spectra similar to those for the comparable cpd clusters. The (Ar)$_1$, $(N_2)_1$, $(CF_4)_1$, and $(C_2F_6)_1$ cluster origins fall at 29 630.2, 29 609.0, 29 622.9, and 29 705.1 cm^{-1}, respectively. The calculated cluster shifts are in good agreement for N_2 and CF_4 clusters, but again are high by a large factor (four, in this case) for the C_2F_6 cluster. Table IV gives this information. Calculated ground state structures for this system are found in Fig. 10 and are as expected, based on the clusters discussed above. Low binding energy isomers can also be found for these systems with the solvent molecule coordinated to the CH_3 group of the radical, but these are dismissed as possible physical cluster structures.

Some spectroscopic features can be identified as arising from the methyl rotational motion for mcpd itself. These are especially obvious in the mcpd(Ar)$_1$ spectrum as all features are doublets as expected for CH_3 nearly free rotation in either the D_0 and D_1 states. Other cluster spectra have additional features associated with the main vibronic bands that can be attributed to both solvent and methyl motion. As for cpd clusters, the z stretch vdW mode is the major vibronic
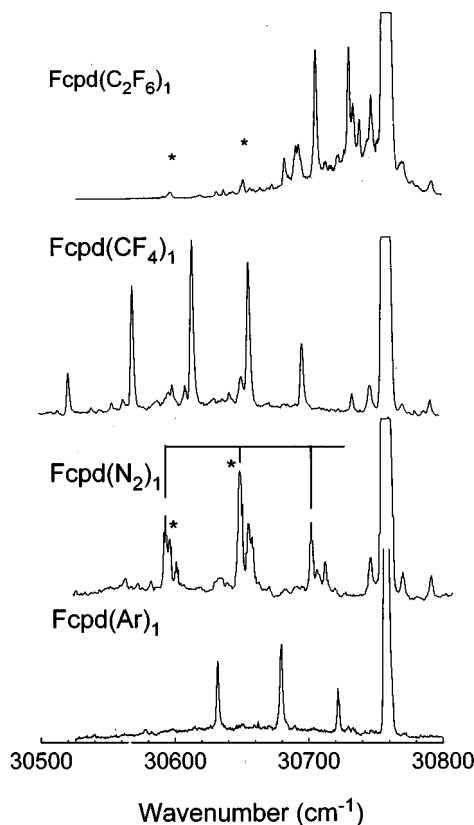
FIG. 11. Fluorescence excitation spectra of Fcpd with Ar, N_2, CH_4, CF_4, and C_2F_6 clusters. Two of the Fcpd(N_2)$_1$ peaks (labeled with asterisks) are coincident with bare radical peaks but can also be assigned as cluster peaks, based on the relative intensities. Asterisks in the Fcpd(C_2F_6)$_1$ spectra indicate bare radical features.

FIG. 12. Calculated structures for Fcpd clusters with Ar, N_2, CH_4, CF_4, and C_2F_6. Fcpd(C_2F_6)$_1$ is the only system that presents two possible isomers.

feature for Ar, N_2, and CF_4 mcpd clusters. The mcpd(C_2F_6)$_1$ cluster seems to suggest ~25 and 32 cm^{-1} features, which may be best assigned by b_y and b_x modes, respectively, but this assignment is not terribly firm.

E. Fcpd/Ar, N_2, CF_4, and C_2F_6 clusters

The cluster spectra for Fcpd are very similar to those found for cpd and mcpd. Figure 11 presents these spectra. The cluster origins lie at 30 632.1, 30 593.7, 30 520.1, and 30 705.9 cm^{-1} for the (Ar)$_1$, (N_2)$_1$, (CF_4)$_1$, and (C_2F_6)$_1$ cluster spectra, respectively. Figure 12 depicts the calculated ground state cluster structures with calculated binding energies given in Table IV. Isomer 1 as before is probably the only observed Fcpd(C_2F_6)$_1$ cluster. With the exception of Fcpd(C_2F_6)$_1$, all shifts are well calculated by the techniques and approximations outlined above, even the especially large one for Fcpd(CF_4)$_1$. The main vdW mode progressions are clearly in σ for Fcpd(Ar)$_1$, (N_2)$_1$, and (CF_4)$_1$ clusters. Table V summarizes these results.

Again the (C_2F_6)$_1$ cluster presents a shift anomaly (-220 cm^{-1} calculated, -52 cm^{-1} observed) and its vibrational progressions appear to be different. The vibronic assignment assumes that the origin of the cluster transition lies at 30 705.9 cm^{-1} and is the first sharp, intense feature in the spectrum, followed by b_y or b_x (25 cm^{-1}) and σ (42 cm^{-1}).
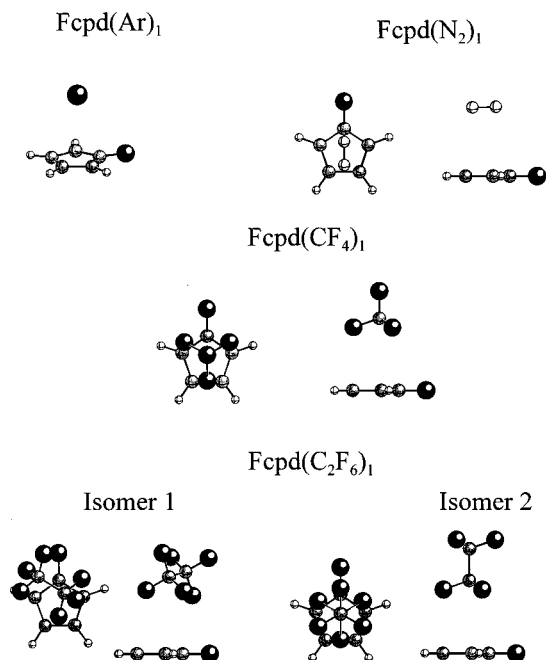
The weak broader features to the low energy side of the origin are probably hot bands.

IV. DISCUSSION

A. Cluster shifts

As pointed out earlier, the cluster spectroscopic shifts for all four Xcpd radical clusters are quite large compared to those found for other aromatic species, either radicals or stable molecules. For example, the cluster shift for aniline (Ar)$_1$ is -40 cm^{-1},[6] for C_6H_5Cl(Ar)$_1$ is -27 cm^{-1},[32] for C_6H_5F(Ar)$_1$ is -24 cm^{-1},[32] and for C_6H_5OH(Ar)$_1$ is -36 cm^{-1}.[32] The Xcpd cluster shifts reported herein are also large compared to those observed for other radicals. For example, the benzyl(Ar)$_1$ shift is -23.8 cm^{-1}.[16] The shifts for Xcpd(Ar)$_1$ fall between -90 and -140 cm^{-1} as given in Table IV.

The shifts reported in this work for Xcpd clusters are similar in magnitude to those found for the Rydberg states of dioxane, DABCO, and ABCO.[33] Ground state binding energies for these latter clusters are relatively small, less than 400 cm^{-1} for Ar$_1$ clusters. Additionally, the benzyl radical(Ar)$_1$[16] cluster has a binding energy of ~400 cm^{-1} in the ground state, not that different than the Xcpd(Ar)$_1$ binding energies given in Table IV. This comparison of shifts and binding energies suggests that the Xcpd cluster shifts arise from a change in atomic parameters comparable to those found for Rydberg states relative to their respective ground states. The atomic parameters α_i and r_i are closely related to atomic charges and atomic volumes.[34] As the change in q_i is not large enough to justify the large shifts, this suggests that the increase in binding energy upon electronic excitation (i.e., the cluster spectroscopic shift) may be due to a large change in atomic volume.

The comparison, presented in Table IV, between excited state binding energies calculated in two different ways (columns $p1$ and $p2$) is instructive. Column $p1$ contains excited state binding energies calculated with excited state atomic charges and geometries for the Xcpd radicals but ground state vdW parameters α_i, r_i. Column $p2$ contains excited state binding energies based on the complete set of vdW parameters, charges, and geometries for excited state Xcpd radicals. vdW parameters are obtained as discussed above based on radical–Ar cluster shift data. From this comparison one can determine that neither the change in atomic charges nor the change in radical geometry is responsible for the cluster spectroscopic shifts. The shift derives from a change in atomic polarizabilities and volumes as expressed (in this instance) through the Lennard-Jones vdW parameters.

The Xcpd radical clusters with C_2F_6 present a surprisingly small shift compared to both the other experimental shifts and the calculated shifts as shown in Table IV. The observed shifts for $Xcpd(C_2F_6)_1$ are all approximately -60 cm^{-1} and those calculated are all -160 to -220 cm^{-1} independent of the isomer structure. One possible explanation for this difference is that the C_2F_6 molecule in the isomer 1 interacts strongly with the hydrogen atoms because of its size (see Figs. 5, 8, 9, and 11). Under this circumstance the determined excited state radical vdW carbon parameters would be incorrect and the hydrogen vdW parameter changes upon excitation would be ignored. The potential surface parameters derived for the $Xcpd(Ar)_1$ cluster fit would thus not apply to $Xcpd(C_2F_6)_1$ clusters.

Cluster shifts are calculated as a difference between two binding energies, $E(D_1)$ and $E(D_0)$, and the excited state binding energy is obtained employing the $Xcpd(Ar)_1$ cluster fitted shift. $cpd(He)_1$ and $cpd(Ne)_1$ clusters have also been investigated and their binding energies and structures have been reported.[17] If the $cpd(Ar)_1$ excited state fitted potential parameters are used to estimate $cpd(He)_1$ and $cpd(Ne)_1$ spectroscopic shifts (-13.7 and -17.0 cm^{-1}, respectively), the calculated shifts are too large by a factor of 3. If, on the other hand, the He and/or Ne cpd cluster data are used to determine the excited state potential parameters, a nearly exact simultaneous fit can be obtained for both $cpd(He)_1$ and $cpd(Ne)_1$ cluster shifts. In this case, however, calculated cluster spectroscopic shifts for $cpd(Ar)_1$, $cpd(Kr)_1$, and $cpd(Xe)_1$ clusters are low by factors of 3, 5, and 7 compared to the experimental shifts[35] -122, -226, and -466 cm^{-1}, respectively. The reason for these discrepancies is clear: Xcpd have very high electron affinities (~ 2.0 eV or greater) and the heavier rare gases have low ionization energies (~ 15 eV or less). Thus, while the $cpd(Ar)_1$ potential fit for the excited state potential parameters of Xcpd makes sense for CH_4, N_2, CF_4, etc., which all have similar ionization energies and polarizabilities to each other and to Ar, it would not make sense for He and Ne clusters with cpd because He and Ne have much higher ionization energies and much lower polarizabilities. The conclusion must follow that the heavier rare gas–cpd clusters contain significant contributions to their binding energies and interactions (especially for excited state Xcpd) from charge transfer.[36]

B. Cluster structures

Calculation of the cluster ground state structure is typically quite reliable because the potential parameters for the interactions are well known and thoroughly tested for many systems.[21] Additionally, the Franck–Condon factors for the cluster vibrational structure strongly suggest that the ground and excited state structures are similar, and that the major change in potential upon D_0 to D_1 excitation is along the z and y directions (see Table I).

The calculated ground state cluster structures are not at all surprising in light of those calculated and determined for the benzyl radical and aromatic molecule clusters found in the literature.[1,2,16,19] One even expects the two structures for $Xcpd(C_2F_6)_1$, based on previously reported aromatic–C_2H_6 cluster structures.[1,31] In the case of $C_6H_5X(C_2H_6)_1$, however, both structures are observed in the supersonic expansion. For $Xcpd(C_2F_6)_1$, HB spectra make clear that only one isomer (presumed to be the lower energy isomer 1) is detected for all Xcpd clusters.

Cluster structures and Xcpd potential energy functions are influenced by the type of ring substitution on the Xcpd radical (i.e., X=H, CH_3, F, CN). The substituent with the largest affect on cluster structure and potential energy is the CN group. The triple bond of the C≡N group changes the cluster structure more than the other substituents due to the delocalization and interaction of the two π-systems of the radical. In all instances the solvent molecule is significantly displaced toward the CN–C_1 position away from the symmetric ring center position. Also the change in parameters upon excitation is similar for the other radicals, but much different for CNcpd. In fact, the same set of excited state C, H parameters can be employed for both cpd and Fcpd; and mcpd parameters are only slightly different from those for cpd. A very different set of potential parameters is needed to generate the CNcpd shifts and these give rise to the unique calculated cluster geometries.

Studies of $cpd(He)_1$ and $cpd(Ne)_1$ clusters[17] suggest that these clusters have the rare gas atom centered over the cpd π-system ring at a z distance of 3.77 Å and 3.58 Å, respectively. The authors of Ref. 17(c) find these separations surprisingly larger. Our ground state structure calculations give 2.98, 3.13, 3.48, 3.61, and 3.79 Å for cpd clustered with He, Ne, Ar, Kr, and Xe, respectively. These latter distances fall directly in place with those of other aromatic molecule–rare gas clusters that are measured and calculated.[19] We cannot explain the reported[17] large equilibrium distances for $cpd(He)_1$ and $cpd(Ne)_1$ except to suggest that large zero point motion and very flat potentials could contribute to the large motionally arranged separations.

C. Cluster vdW modes

The vdW modes identified in these cluster spectra are b_x, b_y, σ: b_x is a translation (bend) that moves the solvent perpendicular to the (y) symmetry axis of Xcpd which goes through the XC_1 bond; b_y is a translation in the y direction toward the substituent; and σ is the z-stretching mode perpendicular to the ring plane. For the CNcpd clusters σ and b_y are the main progression forming modes and b_x is weak if

identified at all. For the F-, H-, CH_3-cpd clusters, σ is the main progression forming mode and b_x and b_y are weak. This trend can be understood based on the potential energy surface parameters presented in Table I. For CNcpd the major parameter changes upon excitation are for the CN group and the ring carbon atoms, but for the other radicals the major changes are only for the ring carbon atoms. Thus, the solvent species move parallel (b_y) and perpendicular (σ) to the ring plane upon CNcpd electronic excitation, but move mostly perpendicular (σ) to the ring plane upon CH_3-, F-, Hcpd electronic excitation.

In general, each cluster has two or three more van der Waals modes that approximately represent torsions (t_i) about the x,y,z axes of the cluster. For symmetric species (N_2, CH_4, etc.), the z-torsional (t_z) motion of the solvent is not highly constrained by the cluster potential energy surface and t_z is best represented as a weakly hindered internal rotor.[1,13,19] For nonsymmetric species, the t_z modes are often of high energy and typically not observed in the van der Waals mode region of the cluster electronic spectra. The t_x and t_y modes are typically the highest energy cluster modes (>100 cm^{-1}) and not observed in cluster vibronic spectra. Two reasons are typically cited for absence of the torsional van der Waals modes in the cluster vibronic spectra: Franck–Condon factors; and poor vibronic coupling to higher energy electric dipole allowed transitions.[37]

In principle, one could employ the van der Waals mode eigenvectors to calculate transition intensities for the vibronic features to check the vibrational assignments which are based on vibrational energy and previous experience with van der Waals mode electronic spectroscopy.[1,13,16,37] Franck–Condon factors and van der Waals mode vibronic coupling[19,37] make this comparison, based only on vibrational mode considerations, not meaningful and beyond the present scope of our understanding of the electronic structure and vibronic interactions for Xcpd radicals and their clusters. Note, too, that strong vibronic coupling interactions are suggested for even the bare Xcpd radicals because of the factor of ~ 10 lifetime shortening observed for higher vibronic states of D_1.[30] Such quantitative calculations are at present not even possible for well-known systems such as benzene–CH_4, N_2, C_2H_6, C_2H_4, H_2O, NH_3, etc.

D. Possible cluster chemistry

A number of pieces of evidence point to the existence of a chemical reaction between the Xcpd radicals in their excited electronic state and methane. The nature of this reaction is an electrophilic radical abstraction of an H atom by cpd to generate cyclopentadiene.

First, the only cluster with CH_4 observed for these radicals is CNcpd(CH_4)$_1$. Since CN stabilizes both the ground and excited electronic configuration through resonance structures, one would expect this system to be the least reactive. Second, the calculated shift for CNcpd(CH_4)$_1$ is almost the only calculated value that is too small. All the other calculated shifts except for CNcpd(N_2)$_1$, for which reaction is not possible, are either very close to the observed value or larger than it. Calculated CH_4 cluster shifts for other (nonreactive)

radicals (e.g., benzyl[16] and NCO[15]) are nearly exactly correct. Third, the CNcpd(Ar)$_1$ cluster demonstrates clear cluster structure at an internal CNcpd vibronic feature at 27 640 cm^{-1}, but CNcpd(CH_4)$_1$ does not. Of course, vibrational dynamics could be responsible for this loss of structure, but the cluster bonding energy is $\sim$700 cm^{-1} in the excited state (640 cm^{-1} is calculated, but the shift is 60 cm^{-1} too small) and the cluster is probably still bound at this energy even if the vibrational redistribution is rapid.[6] Thus, the suggestion is that $\sim$600 cm^{-1} of excess vibrational energy in the D_1 state is sufficient to cause the reaction to occur (i.e., E_{act} $<$600 cm^{-1} on the D_1 radical surface). Fourth, the appearance of the CNcpd(CH_4)$_1$ and CNcpd(CD_4)$_1$ spectra is unique for this cluster system, and even for other CH_4 clusters of aromatic radicals and aromatic stable molecules. In all instances of which we are aware, for one-to-one methane clusters with chromophores that are not reactive in either their ground or first excited electronic states, cluster spectra are sharp and well defined, and the CD_4 and CH_4 spectra are quite similar.[1,33] Clearly this is not the case for CNcpd(CH_4)$_1$ and CNcpd(CD_4)$_1$. Indeed, the two spectra are different and appear to have $\sim$35 cm^{-1} different cluster shift (see Table IV). This shift difference may not be a correct representation and may simply arise from different spectroscopic intensities or Franck–Condon factors, but the character of the two spectra is quite different. Many of the features in the CH_4 cluster spectrum are due to methane rotation above the ring and one expects to find poorer resolution in the CNcpd(CD_4)$_1$ spectrum than in the CNcpd(CH_4)$_1$ spectrum. Nonetheless, such loss of structure, the broad background, and crowded spectrum are all spectroscopic characteristics that can be associated with a chromophore undergoing chemical reaction but confined to the reactant side of a small ($<$600 cm^{-1}) barrier.

The above four points or observations only suggest that a chemical reaction for Xcpd–methane clusters can occur. If this is true, the reaction has just begun for CNcpd(CH_4)$_1$ and CNcpd(CD_4)$_1$, on the D_1 potential energy surface, but has proceeded further for the other Xcpd (X=H, F, CH_3) radicals. If the reaction does indeed occur, the radical reactivity would be in the order mcpd$\sim$cpd$>$Fcpd$\gg$CNcpd, for an electrophilic radical abstraction of an H atom. Additionally, CH_4 would be more reactive in this regard than CH_3F, CH_2F_2, CHF_3, etc., because the H atoms of methane would have a higher electron density than those of halogen substituted methanes; of course, methyl substituted methanes would be still more reactive toward H atom abstraction than methane itself. By adding more F atoms to methane, one can generate a reactivity scale for the reaction partner. The results of these experiments will be presented in paper III of this series, but their general behavior is consistent with the above trends and analysis. The most consistent and simple explanation of this data set is that an incipient chemical bond forms in the D_1 state of Xcpd radicals clustered with methane and halo substituted methanes.

A properly crafted experiment, in which the photolysis and clustering processes are spatially separated, would also allow the search for the CH_3 radical formed from this reaction.

V. CONCLUSIONS

Substituted cyclopentadienyl radicals can be readily clustered with simple atomic, diatomic, and polyatomic solvent species and their cluster vibronic spectra obtained. These spectra have many common features: The two most important are (1) that all clusters have much larger spectroscopic shifts than other comparable aromatic molecule or radical species–solvent clusters, and (2) that the most prevalent van der Waals modes in the spectra are the z-stretch (σ), the y-bend (b_y) and the x-bend (b_x). Calculated cluster structure shows that, considering van der Waals and Coulomb interactions, the CN substituent has the most significant effect on the position of solvent species with respect to displacement from the ring center. Vibronic features for the CNcpd clusters tend to be b_y bends and σ stretches, while those for the other radicals (Fcpd, cpd, mcpd) tend to be only σ stretches.

Ab initio calculations are presented to obtain ground and excited state atomic charges for the radicals in order to generate potential parameters to obtain vdW modes, binding energies, and cluster structures. The calculations are checked by transition energies for the $D_1 \leftarrow D_0$ bare radical transitions and structures. Ground state solvent calculations are also performed to get atomic charges. Charges are a function of the basis set chosen and the method of calculating the charges from the obtained wave function. The method that gives converged results for good basis sets (larger than 6-31G**) is the potential grid algorithm.

Atom–atom potential energy calculations reproduce fairly accurately the observed cluster spectroscopic shifts, except for CNcpd(N$_2$)$_1$ and CNcpd(CH$_4$)$_1$ clusters, and for Xcpd(C$_2$F$_6$)$_1$ clusters. We suggest that the latter large solvent molecule does not conform to the approximations used to obtain excited state carbon parameters for the van der Waals terms in the interaction potential. In general, however, the approach taken to obtain an excited state potential surface for the radical [that is, calculating charges, fitting carbon, and substituent potential parameters to the Xcpd(Ar)$_1$ shift] is a reasonable qualitative technique.

The potentials thus obtained and verified seem to give qualitative values for ground and excited state vdW modes for the clusters. These calculations are sufficient to generate tentative vdW mode assignments for the observed cluster vibronic structures.

We present arguments that the Xcpd(CH$_4$)$_1$ clusters can react on the excited state cluster potential surface, based on several observations: (1) Only the CNcpd(CH$_4$)$_1$ cluster is observed; (2) CNcpd(CH$_4$)$_1$ and CNcpd(CD$_4$)$_1$ spectra are broad; (3) CNcpd(CH$_4$)$_1$ and (CD$_4$)$_1$ show very large spectroscopic cluster shifts (much larger than calculated); and (4) these spectra are completely different from other aromatic molecule and radical–methane cluster spectra. Paper III of this series presents more detail and systematic experimental and theoretical data dealing with the Xcpd–CH$_4$ excited state chemistry.

[1] R. Pereira, T. Calvo, F. Castaño, and M. T. Martínez, Chem. Phys. **201**, 433 (1995); M. Schauer and E. R. Bernstein, J. Chem. Phys. **82**, 726 (1985); S. M. Beck, M. G. Liverman, L. L. Monts, and R. E. Smalley, *ibid.* **70**, 232 (1979); R. E. Smalley, L. Wharton, D. H. Levy, and D. W. Chandler, *ibid.* **68**, 2487 (1978); R. Pereira, I. Álava, F. Castaño, and M. T. Martínez, J. Chem. Soc., Faraday Trans. **90**, 2443 (1994); S. Sun and E. R. Bernstein, J. Phys. Chem. **100**, 11348 (1996), and references therein; M. C. Heaven, Annu. Rev. Phys. Chem. **43**, 283 (1992); E. R. Bernstein, in *Atomic and Molecular Clusters*, edited by E. R. Bernstein (Elsevier, New York, 1990), p. 551.

[2] J.-G. Jäckel, R. Schmid, H. Jones, T. Nakanaga, and H. Takeo, Chem. Phys. **215**, 291 (1997); R. Nowak, J. A. Menapace, and E. R. Bernstein, J. Chem. Phys. **89**, 1309 (1988); Th. Brupbacher and A. Bauder, *ibid.* **99**, 9394 (1993); J. Wanna, J. A. Menapace, and E. R. Bernstein, *ibid.* **85**, 1795 (1986); O. K. Abou-Zied, H. K. Sinha, and R. P. Steer, *ibid.* **101**, 7989 (1997).

[3] Th. Weber, A. M. Smith, E. Riedle, H. J. Neuser, and E. W. Schlag, Chem. Phys. Lett. **175**, 79 (1990); P. Hobza, O. Bludsky, H. L. Selzle, and E. W. Schlag, J. Chem. Phys. **98**, 6223 (1993); Y. Ohshima, H. Kohguchi, and H. Endo, Chem. Phys. Lett. **184**, 21 (1991).

[4] E. J. Bieske, M. W. Rainbird, I. M. Atkinson, and A. E. W. Knight, J. Chem. Phys. **91**, 752 (1989), and references therein; S. Li and E. R. Bernstein, *ibid.* **95**, 1577 (1991).

[5] Chakravarty, D. C. Clary, A. D. Esposti, and H.-J. Werner, J. Chem. Phys. **95**, 8149 (1991); **93**, 3367 (1990).

[6] M. F. Hineman, S. K. Kim, E. R. Bernstein, and D. F. Kelley, J. Chem. Phys. **96**, 4904 (1992); B. Coutant and P. Brechignac, *ibid.* **91**, 1978 (1989); M. R. Nimlos, M. A. Young, E. R. Bernstein and D. F. Kelley, *ibid.* **91**, 5268 (1989).

[7] H. Bürger, Angew Chem. Int. Ed. Engl. **36**, 718 (1997); T. Emilsson, T. D. Klots, R. S. Ruoff, and H. S. Gutowsky, J. Chem. Phys. **93**, 6972 (1990), and references therein; M. Hineman, E. R. Bernstein, and D. F. Kelley, *ibid.* **101**, 850 (1994); M. Hineman, E. R. Bernstein, and D. F. Kelley, *ibid.* **98**, 2516 (1993).

[8] See for example Ref. 1; E. R. Bernstein, Annu. Rev. Phys. Chem. **46**, 197 (1995); Q. Y. Shang and E. R. Bernstein, Chem. Rev. **94**, 2015 (1994); M. I. Lester, Adv. Chem. Phys. **96**, 51 (1996); *Chemical Reactions in Clusters*, edited by E. R. Bernstein (Oxford University Press, N. Y. 1996); P. Hobza, H. L. Selzle, and E. W. Schlag, Chem. Rev. **94**, 1767 (1994); P. Hobza and R. Zahradnik, *ibid.* **88**, 871 (1988); A. D. Buckingham, P. W. Fowler, and J. M. Hutson, *ibid.* **88**, 963 (1988); P. W. Joireman, S. M. Ohline, and P. M. Felker, J. Phys. Chem. A **102**, 4481 (1998).

[9] D. Fulle, H. F. Hamann, H. Hippler, and J. Troe, J. Chem. Phys. **105**, 983 (1996); R. A. Loomis, R. L. Schwartz, and M. I. Lester, *ibid.* **104**, 6984 (1996); W. M. Fawzy and M. C. Heaven, *ibid.* **92**, 909 (1990); J. L. Lemaire, W.-Ü. L. Tchang-Brillet, N. Shafizadeh, F. Rostas, and J. Rostas, *ibid.* **91**, 6657 (1989).

[10] R. W. Randall, C. Chuang, and M. I. Lester, Chem. Phys. Lett. **200**, 113 (1992); M. J. McQuaid, G. W. Lemire, and R. C. Sausa, *ibid.* **210**, 350 (1993); G. W. Lemire, M. J. McQuaid, and R. C. Sausa, J. Chem. Phys. **99**, 91 (1993).

[11] W. G. Lawrence, Y. Chen, and M. C. Heaven, J. Chem. Phys. **107**, 7163 (1997); M. Yang and M. H. Alexander, *ibid.* **107**, 7148 (1997), and references therein.

[12] L. J. van de Burgt and M. C. Heaven, J. Chem. Phys. **89**, 2768 (1988).

[13] L. Yu, J. Williamson, S. C. Foster, and T. A. Miller, J. Chem. Phys. **97**, 5273 (1992); S. Sun and E. R. Bernstein, *ibid.* **103**, 4447 (1995).

[14] J. A. Fernández, J. Yao, and E. R. Bernstein, J. Chem. Phys. **107**, 3363 (1997).

[15] J. Yao, J. A. Fernández, and E. R. Bernstein, J. Chem. Phys. **107**, 8813 (1997).

[16] R. Disselkamp and E. R. Bernstein, J. Chem. Phys. **98**, 4339 (1993); J. Phys. Chem. **98**, 7260 (1994); H. S. Im and E. R. Bernstein, J. Chem. Phys. **95**, 6326 (1991).

[17] L. Yu, S. C. Foster, J. M. Williamson, M. C. Heaven, and T. A. Miller, J. Phys. Chem. **92**, 4263 (1988); L. Yu, D. W. Cullin, J. M. Williamson, and T. A. Miller, J. Chem. Phys. **95**, 804 (1991); D. W. Cullin, L. Yu, J. M.

Williamson, and T. A. Miller, J. Phys. Chem. **96**, 89 (1992).

[18] R. O. Lindsay and C. F. H. Allen, *Organic Syntheses Collective*, edited by E. C. Horning (Wiley, London, 1995), pp. 710–711.

[19] R. Nowak, J. A. Menapace, and E. R. Bernstein, J. Chem. Phys. **89**, 1309 (1988); Th. Brupbacher, J. Makarewicz, and A. Bauder, *ibid.* **101**, 9736 (1994); W. Lu, Y. Hu, and S. Yang, *ibid.* **108**, 12 (1998); J. A. Fernandez and E. R. Bernstein, *ibid.* **106**, 3029 (1997); O. K. Abou-Zied, H. K. Sinha, and R. P. Steer, J. Phys. Chem. **100**, 4375 (1996); H. K. Sinha and R. P. Steer, J. Mol. Spectrosc. **181**, 194 (1997), and references therein; M. Coreno, S. Piccirillo, A. Giardini Guidoni, A. Mele, A. Palleshi, P. Brechignac, and P. Parneix, Chem. Phys. Lett. **236**, 580 (1995); N. M. Lakin, G. Pietraperia, M. Becucci, E. Castellucci, M. Coreno, A. Giardini Guidoni, and A. van der Avoird, J. Chem. Phys. **108**, 1836 (1998); S. Leutwyler, *ibid.* **81**, 5480 (1984); S. Leutwyler and J. Jortner, J. Phys. Chem. **91**, 5558 (1987); E. Shalev, N. Ben-Horin, U. Even, and J. Jortner, J. Chem. Phys. **95**, 3147 (1991); J. Jortner, U. Even, S. Leutwyler, and Z. Berkovitch-Yellin, *ibid.* **78**, 308 (1981).

[20] E. R. Bernstein, J. Chem. Phys. **52**, 4701 (1970); G. W. Robinson, Annu. Rev. Phys. Chem. **21**, 429 (1970).

[21] R. A. Scott and H. A. Scheraga, J. Chem. Phys. **45**, 2091 (1966); F. A. Momany, L. M. Carruthers, R. F. McGuire, and H. A. Scheraga, J. Phys. Chem. **78**, 1595 (1974); F. A. Momany, R. F. McGuire, A. W. Burgess, and H. A. Scheraga, *ibid.* **79**, 2361 (1975); G. Némethy, M. S. Pottle, and H. A. Scheraga, *ibid.* **87**, 1883 (1988); R. A. Scott and H. A. Scheraga, J. Chem. Phys. **42**, 2209 (1965); K. S. Pitzer, Adv. Chem. Phys. **2**, 59 (1959); K. S. Pitzer, J. Am. Chem. Soc. **78**, 4565 (1956).

[22] GAUSSIAN 94, M. J. Frisch, G. W. Trucks, H. B. Schlegel, P. M. W. Gill, B. G. Johnson, M. A. Robb, J. R. Cheeseman, T. A. Keith, G. A. Petersson, J. A. Montgomery, K. Raghavachari, M. A. Al-Laham, V. G. Zakrzewski, J. V. Ortiz, J. B. Foresman, J. Cioslowski, B. B. Stefanov, A. Nanay-akkara, M. Challacombe, C. Y. Peng, P. Y. Ayala, W. Chen, M. W. Wong, J. L. Andrés, E. S. Replogle, R. Gomperts, R. L. Martin, D. J. Fox, J. S. Binkley, D. J. Defrees, J. Baker, J. P. Stewart, M. Head-Gordon, C. González, and J. A. Pople, Gaussian Inc., Pittsburgh, PA, 1995.

[23] L. Yu, D. W. Cullin, J. M. Williamson, and T. A. Miller, J. Chem. Phys. **98**, 2682 (1993).

[24] J. Casado, L. Nygaard, and G. O. Sorensen, J. Mol. Struct. **8**, 211 (1971).

[25] D. W. Cullin, L. Yu, J. M. Williamson, M. S. Platz, and T. A. Miller, J. Phys. Chem. **94**, 3387 (1990).

[26] L. Yu, J. M. Williamson, and T. A. Miller, Chem. Phys. Lett. **162**, 431 (1989).

[27] C. M. Breneman and K. B. Wiberg, J. Comput. Chem. **11**, 361 (1990).

[28] E. B. Wilson, J. C. Decius, and P. C. Cross, *Molecular Vibrations* (Dover, New York, 1980); J. A. Fernandez and E. R. Bernstein, J. Chem. Phys. **106**, 3029 (1997).

[29] Note that, in order for the vibrational assignments for the clusters to be consistent, we have maintained the axis system of Table I for all Xcpd molecules. Thus, the electronic transition for the low symmetry Xcpds is labeled $^2B_1 \leftarrow {}^2B_1$ rather than the more usual axis arrangement $^2B_2 \leftarrow {}^2B_2$ as given in Ref. 17. Moreover, because the ground state of cpd is $^2E_1''$, the ''true D_1 state'' for these lower symmetry radicals is in the infrared and not observed. The optical transition that is $D_1 \leftarrow D_0$ for cpd is actually $D_2 \leftarrow D_0$ for low symmetry Xcpds. We ignore this irrelevant subtlety in the text.

[30] F. Di Mauro, M. Heaven, and T. A. Miller, Chem. Phys. Lett. **124**, 489 (1986).

[31] M. Schawer, K. S. Law, and E. R. Bernstein, J. Chem. Phys. **82**, 736 (1985).

[32] E. J. Bieske, M. W. Rainbird, I. M. Atkins, and A. E. W. Knight, J. Chem. Phys. **91**, 752 (1989).

[33] P. Moreno, Q.-Y. Shang, and E. R. Bernstein, J. Chem. Phys. **97**, 2869 (1992); Q. Y. Shang, P. O. Moreno, S. Li, and E. R. Bernstein, *ibid.* **98**, 1876 (1993); Q. Y. Shang, P. O. Moreno, C. Dion, and E. R. Bernstein, *ibid.* **98**, 6769 (1993); Q. Y. Shang, P. O. Moreno, and E. R. Bernstein, J. Am. Chem. Soc. **116**, 302 (1994); **116**, 311 (1994).

[34] J. K. Badenhoop and F. Weinhold, J. Chem. Phys. **107**, 5422 (1997); K. E. Laidig and R. F. W. Bader, *ibid.* **93**, 7213 (1990).

[35] J. Yao and E. R. Bernstein (unpublished).

[36] A. J. Stone, *Theory of Intermolecular Forces* (Oxford University Press, Oxford, 1997).

[37] J. A. Menapace and E. R. Bernstein, J. Phys. Chem. **91**, 2533 (1987).